



Mariusz Tasior | Ilko Bald | Irena Deperasińska | Piotr J. Cywiński
Daniel T. Gryko

An internal charge transfer-dependent solvent effect in V-shaped azacyanines

Suggested citation referring to the original publication:

Org. Biomol. Chem. 13 (2015), pp. 11714–11720

DOI <http://dx.doi.org/10.1039/c5ob01633a>

ISSN (online) 1477-0539

ISSN (print) 1477-0520

Postprint archived at the Institutional Repository of the Potsdam University in:

Postprints der Universität Potsdam

Mathematisch-Naturwissenschaftliche Reihe ; 306

ISSN 1866-8372

<http://nbn-resolving.de/urn:nbn:de:kobv:517-opus4-102704>



Cite this: *Org. Biomol. Chem.*, 2015, **13**, 11714

An internal charge transfer-dependent solvent effect in V-shaped azacyanines†

Mariusz Tasiór,^a Ilko Bald,^{b,c} Irena Deperasińska,^d Piotr J. Cywiński*^{e,f} and Daniel T. Gryko*^a

New V-shaped non-centrosymmetric dyes, possessing a strongly electron-deficient azacyanine core, have been synthesized based on a straightforward two-step approach. The key step in this synthesis involves palladium-catalysed cross-coupling of dibromo-*N,N'*-methylene-2,2'-azapyridinocyanines with arylacetylenes. The resulting strongly polarized π -expanded heterocycles exhibit bright green to orange fluorescence and they strongly respond to changes in solvent polarity. We demonstrate that differently electron-donating peripheral groups have a significant influence on the internal charge transfer, hence on the solvent effect and fluorescence quantum yield. TD-DFT calculations confirm that, in contrast to the previously studied bis(styryl)azacyanines, the proximity of S_1 and T_2 states calculated for compounds bearing two 4-*N,N*-dimethylaminophenylethynyl moieties establishes good conditions for efficient intersystem crossing and is responsible for its low fluorescence quantum yield. Non-linear properties have also been determined for new azacyanines and the results show that depending on peripheral groups, the synthesized dyes exhibit small to large two-photon absorption cross sections reaching 4000 GM.

Received 5th August 2015,
Accepted 7th October 2015

DOI: 10.1039/c5ob01633a

www.rsc.org/obc

Introduction

The discovery of the relationship between structure and non linear optical properties has provided new possibilities for the application of two-photon absorbing organic materials in various fields.^{1–5} Rationally designed two-photon absorbing materials are widely used in optical power limiting,⁶ 3D micro-fabrication,⁷ 3D data storage,^{8,9} localized release of bio-active species¹⁰ and multiphoton microscopy.¹¹ Particularly, the latter technique was proved to be useful in bioimaging, due to the high spatial resolution and low excitation energy.¹²

In order to achieve a strong, two-photon-induced optical response, the following structural motifs are usually employed:

D- π -A dipoles, D- π -A- π -D quadrupoles and more complex (D- π)₃A octupoles (where D and A denote respectively electron donors and acceptors and ' π ' is a π -conjugated bridge), however materials based on porphyrins,^{13,14} multi-annulenes,¹⁵ polymers and nano-aggregates¹⁶ have also been extensively studied. Arylamines are the most frequently used structural motif playing the role of an electron donor, whereas many different electron acceptors have been tested. Cyano-, nitro- and polyfluoro-substituted benzene derivatives, azines, azoles, squaraine dyes,¹⁷ coumarins,¹⁸ diketopyrrolo-pyrroles,^{19,20} and merocyanines²¹ have already been proven to strongly enhance the two-photon action, but new electron acceptors are continuously developed. Needless to say, the obvious candidates for electron-deficient units are quaternary salts of six-membered aza-heterocycles, compounds predominantly studied by Vaquero and co-workers.²² We recently contributed to this subject by introducing π -expanded azacyanine dyes into two-photon absorbing scaffolds.²³ There are several features that make *N,N'*-methylene-2,2'-azapyridinocyanines particularly interesting compounds for donor-acceptor systems: straightforward synthesis,^{24–27} large two-photon brightness and, finally, good solubility in polar solvents, including aqueous solutions. The latter property can be attributed to the cationic structure and should be considered as a great advantage over many other two-photon absorbing dyes being usually poorly water soluble π -expanded systems. Moreover, the non-linear absorption of the previously presented bis(styryl)azacyanines²³ occurs in the so-called “biological

^aInstitute of Organic Chemistry, Polish Academy of Sciences, Kasprzaka 44/52, 01-224 Warsaw, Poland. E-mail: dtgryko@icho.edu.pl

^bDepartment of Chemistry, University of Potsdam, Karl-Liebknecht-Strasse 24–25, 14476 Potsdam, Germany

^cBAM Federal Institute of Materials Research and Testing, Richard-Willstätter Strasse 11, 12489 Berlin, Germany

^dInstitute of Physics, Polish Academy of Sciences, Al. Lotników 32/46, 02-668 Warsaw, Poland

^eFunctional Materials and Devices, Fraunhofer Institute for Applied Polymer Research, Geiselbergstrasse 69, 14476 Potsdam, Germany. E-mail: pcywinski@ichf.edu.pl

^fInstitute of Physical Chemistry, Polish Academy of Sciences, Kasprzaka 44/52, 01-224 Warsaw, Poland

†Electronic supplementary information (ESI) available: Copies of ¹H and ¹³C NMR spectra as well as fluorescence decays for compounds **4** and **5**. See DOI: 10.1039/c5ob01633a

window”, while their cationic character might favour a specific interaction with particular subcellular components. Taking all the above into consideration, π -expanded azacyanines seem to be promising candidates for applications in two-photon bio-imaging, therefore we decided to further explore their properties. Herein, we would like to present the synthesis and photophysical properties of new bis(phenylethynyl)azacyanines.

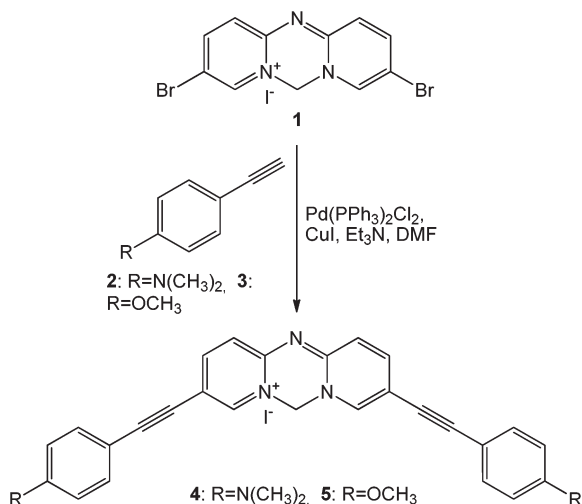
Results and discussion

Design and synthesis

Azacyanines are considered to be strong electron acceptors; therefore, their substitution with strong electron donors *via* a π -bridge should result in the formation of a typical quadrupolar D- π -A⁺- π -D structure. To achieve this goal, we decided to follow palladium catalyzed Sonogashira-type coupling of 3,9-dibromoazacyanine **1** with phenylacetylenes **2** and **3**, substituted with electron-donating groups on the phenyl ring (Scheme 1). All our previous attempts^{2,3} resulted in the formation of a complex mixture; however the palladium/copper catalytic system in DMF²²ⁱ finally led to expected products **4** and **5**. Despite the formation of multiple side-products, careful chromatography and crystallization led to analytically pure samples. The prepared dyes were chemically stable and were subjected to photophysical studies.

Photophysical properties

Steady-state spectroscopy. The electronic absorption and steady-state fluorescence spectra obtained for compounds **4** and **5** are shown in Fig. 1 and in Fig. 2 and the corresponding parameters are shown in Table 1. In comparison with the parent 2,10-dimethylazacyanine, which exhibits absorption and emission maxima at 388 and 452 nm respectively,^{2,3} both azacyanines **4** and **5** have their absorption and emission maxima bathochromically shifted by *ca.* 100 nm (see also Fig. S1 and S2 in the ESI[†]). The current dyes **4** and **5** differ



Scheme 1 The synthesis route used to obtain azacyanines **4** and **5**.

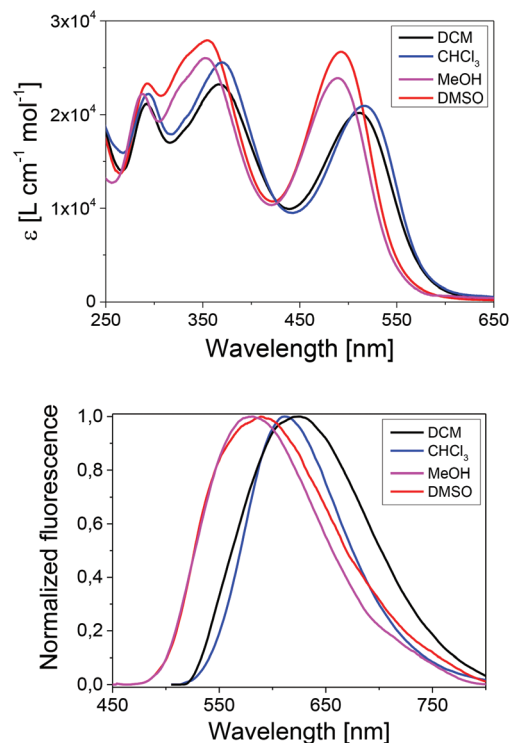


Fig. 1 Electronic absorption spectra (top) and normalized fluorescence emission spectra (bottom, $\lambda_{\text{ex}} = 490$ nm) collected for **4** in all the studied solvents.

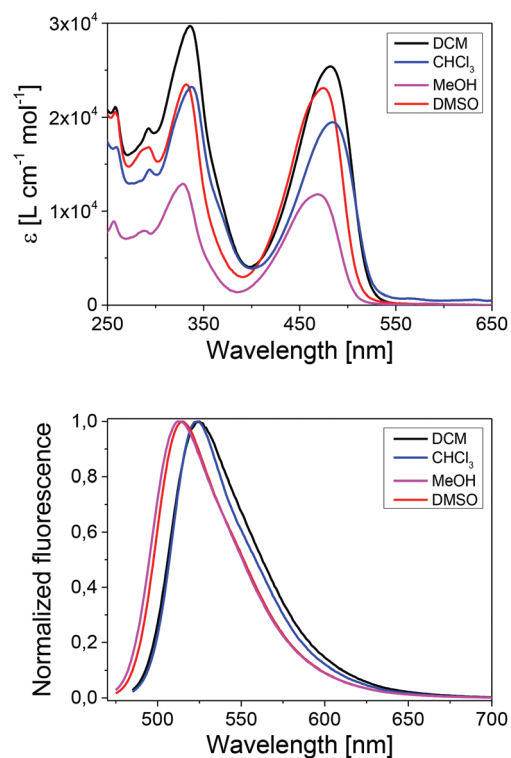


Fig. 2 Electronic absorption spectra (top) and normalized fluorescence emission spectra (bottom, $\lambda_{\text{ex}} = 470$ nm) collected for **5** in all the studied solvents.

Table 1 Basic photophysical properties determined for **4** and **5** from steady-state experiments. λ_{abs} is the wavelength of the absorption peak, ϵ is the molar extinction coefficient determined at λ_{abs} , λ_{ex} is the excitation wavelength, λ_{em} is the wavelength of the fluorescence emission peak, $\Delta\nu$ is Stokes' shift and Φ_{fl} is the fluorescence quantum yield

Dye	λ_{abs} (nm)	$\epsilon \times 10^{-3}$ ($\text{M}^{-1} \text{cm}^{-1}$)	λ_{em} (nm)		$\Delta\nu$ (cm^{-1})	Φ_{fl} (%)
			λ_{ex1}^a	λ_{ex2}^b		
4 (CH_2Cl_2)	293	21	414	626	3600	1.0
	368	23	490			
	510	20	616			
4 (CHCl_3)	294	22	406	611	3000	3.1
	370	25.5	463			
	517	21	614			
4 (DMSO)	292	33.5	435	589	3300	0.5
	355	40 ^c	463			
	492	38				
4 (MeOH)	288	22	426	580	3200	0.4
	352	26 ^c	463			
	490	24	570			
5 (CH_2Cl_2)	293	19	380	525	1700	26
	336	30	400			
	482	25	524			
5 (CHCl_3)	294	14.5	524	524	1600	41
	337	23.2				
	484	19.5				
5 (DMSO)	293	17	515	515	1700	53
	332	23.5				
	474	23				
5 (MeOH)	288	8	512	512	1700	46
	330	13				
	470	12				

^a **4** was excited at 330 nm and **5** at 350 nm. ^b **4** was excited at 470 nm and **5** at 490 nm. ^c At a shoulder at around 300 nm.

from the previously published ones²³ in the type of linker, in which the C–C triple bond is replaced by the C–C double bond. As shown by Meier²⁸ and Blanchard-Desce²⁹ such a difference can have a profound effect on both linear and non-linear optical properties. In particular, it was found that the ethylene linker ensures improved conjugation between various parts of the molecule leading typically to a stronger bathochromic shift, a larger two-photon absorption cross-section and higher quantum yields.^{28,29} In our case however, the comparison of optical properties of dyes **4** and **5** reveals that both their

absorption and emission are bathochromically shifted *versus* those of their analogues bearing the C–C double bond²³ and the typical difference is ~ 20 nm. What is more intriguing is that while fluorescence quantum yields for both dyes possessing MeOC_6H_4 groups are reasonably high (41% and 19%²³ respectively in CHCl_3) there is a striking difference for their analogues possessing more electron-donating $\text{Me}_2\text{NC}_6\text{H}_4$ groups. Indeed, while the fluorescence quantum yield for the previously studied compound bearing the ethylene linker was 25%,²³ Φ_{fl} for dye **4** is only 3.1% in CHCl_3 (Table 1). The effect of solvent polarity on the emission intensity is also profound. Dimethoxy-substituted cyanine **5** retains a high fluorescence quantum yield ($\Phi_{\text{fl}} = 0.53$ in DMSO) characteristic of 2,10-dimethylazacyanine ($\Phi_{\text{fl}} = 0.44$ in H_2O), whereas the fluorescence of dimethylamino-substituted cyanine **4** is strongly quenched ($\Phi_{\text{fl}} = 0.05$ in DMSO).

In order to reveal the reason for such a striking difference, we measured the absorption and emission spectra of **4** and **5** in four solvents of different polarities (Table 2). We observed a strong negative solvatochromism for both dyes (analogous to classical Brooker's merocyanine³⁰), indicating larger stabilization of the ground state of azacyanine molecules combined with increased reorganization energy in more polar solvents, which thus increases the energy gap between the ground state and the (Franck–Condon) excited state and leads to a shorter wavelength of the absorbed light. This effect was particularly strong for **4**, where 20 and 46 nm hypsochromic shifts of respectively absorption and emission maxima were observed in the polarity range between dichloromethane and methanol.

Time-resolved spectroscopy. In order to provide further insight into the mechanism of fluorescence quenching observed for compound **4**, we executed time-resolved fluorescence spectroscopy measurements. The fluorescence decays are presented in Fig. 3 (top) and (bottom) and the corresponding fit parameters in Table 2. The results revealed that the fluorescence decay time of azacyanine **5** is virtually unaffected by changes in solvent polarity ($\tau_1 = 2.5$ ns), whereas the fluorescence decay time determined for **4** is shortened in solvents of low polarity. Noticeably, two contributions could be determined: the first shorter ($\tau_1 = 0.8$ – 1.8 ns) for the locally

Table 2 Basic photophysical properties determined for **4** and **5** from time-resolved experiments. A_1 and A_2 is respectively the contribution of decay times τ_1 and τ_2 in the fluorescence decay, τ_{av} is an average decay time calculated based on τ_1 and τ_2 values, k_{r} and k_{nr} is the rate of radiative and non-radiative processes, respectively

Compd.	λ_{em} (nm)	A_1 (%)	τ_1 (ns)	A_2 (%)	τ_2 (ns)	τ_{av} (ns)	k_{r} (10^8 s^{-1})	k_{nr} (10^8 s^{-1})
4 ^a	490	86	1.85	14	7.55	2.6	0.04	3.73
4 ^b	410	97	0.8	3	4.5	0.9	0.34	10.76
	615	98	0.6	2	6.2	0.7	0.44	13.84
4 ^c	460	90	1.45	10	10	2.3	0.02	4.33
4 ^d	430	20	1.3	80	5.9	5.0	0.08	1.99
5 ^a	520	100	2.5	—	—	2.5	1.04	2.96
5 ^b	520	100	2.5	—	—	2.5	1.64	2.36
5 ^c	520	100	2.6	—	—	2.6	2.04	1.81
5 ^d	520	100	2.4	—	—	2.4	1.91	2.25

^a Measured in CH_2Cl_2 . ^b Measured in CHCl_3 . ^c Measured in DMSO. ^d Measured in MeOH.

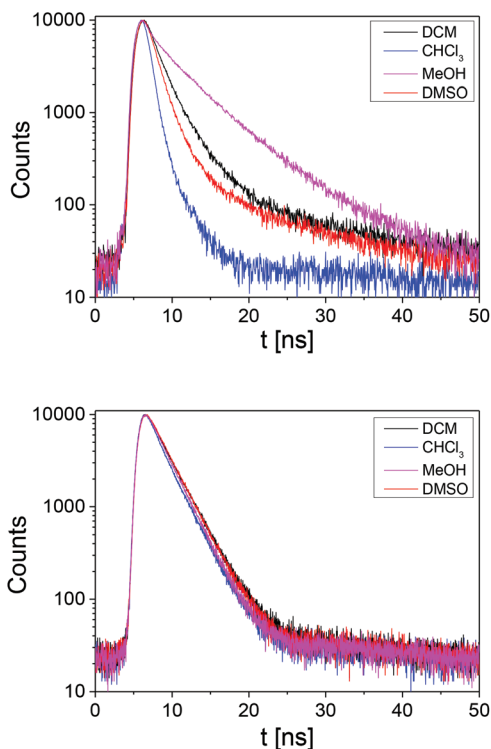


Fig. 3 Fluorescence decays collected for compounds 4 (top) and 5 (bottom) in four solvents of different polarities.

excited state and the second longer ($\tau_2 = 5\text{--}10$ ns), which can be associated with the internal charge-transfer state.

As can be seen in Table 2, in moderately low polarity solvents the major decay time contribution comes from a short living species decaying from a locally excited state, while for much more polar solvents such as methanol the longer component associated with internal charge transfer is dominating. In the case of methanol an additional effect associated with hydrogen bonding may have an influence on the final decay time.

In multifluorophoric systems a charge separation may occur depending on the solvent polarity and fluorescence emission can be observed before and after the charge separation. In this case, the loss in quantum yield can be an effect of internal charge transfer. In low polarity solvents the dye emits at shorter wavelengths from the locally excited state, but as the solvent polarity increases the fluorescence from the internal charge-transfer state becomes visible at longer wavelengths.³¹ Simultaneously, the quantum yield decreases significantly for 4 when compared with 5 for which ICT was observed only in the case of rather low polar DCM. Additionally, two contributions are observed in fluorescence decay, which again can be assigned to ICT.

Theoretical calculations

To strengthen optical data interpretation, we decided to perform DFT calculations, including optimization of the structures of compounds 4 and 5 (as well as two previously reported

bis(styryl)azacyanines²³) in the ground and excited electronic states and the determination of the energy of electronic transitions that characterize them (Tables S1–S3†). The results of TD-DFT B3LYP/6-31G(d,p) calculations of transition energies and oscillator strengths for compounds 4 and 5 are shown in Table S2,† while Table S3† presents the results obtained for the structures optimized in the excited state.

A comparison of the calculated transition energies with the experimental data shows that they are subject to systematic error, typical of the TD-DFT B3LYP method applied to charge transfer systems.³² These deviations have been an object of rational systematization in terms of the type of investigated molecular system.³² In the case of the V-shaped azacyanines, the calculated energies of S_1 states are too low by *ca.* 1500 cm^{-1} – 3000 cm^{-1} . On the other hand, the calculations well reproduce the distribution of the band intensity in the observed absorption spectra, which is shown in Fig. S3.† Theoretical results correctly reflect the experimentally determined relationship between the absorption wavelengths corresponding to the individual molecules: $\lambda_{\text{abs}}(-\text{NMe}_2) > \lambda_{\text{abs}}(-\text{OCH}_3)$ for bis(phenylethynyl) and bis(styryl)²³ substituted azacyanines.

In the view of the data shown in Tables 3 (with the use of 4 as an example) and S2,† the substituent effect on the electronic spectra of V-shaped azacyanines is correlated with the electronic charge transferred from D groups to A groups at the excitation, which confirms the intuitive knowledge on the internal charge-transfer (ICT) properties of the studied systems. The calculation results qualitatively reproduce the

Table 3 Charge transfer character of the $S_0 \rightarrow S_1$ transition in V-shaped azacyanines, the results of DFT B3LYP/6-31G(d,p) calculations for 4 in CH_2Cl_2 . $S_0 \rightarrow S_1$ transition is described by the electronic configuration (HOMO, LUMO), showed at the top. $q(S_0)$ and $q(S_1)$ characterize the distributions of charge over individual subgroups of molecules (shown above) in the ground and excited states, respectively. The δq values are the differences between them. It is seen that electronic charge $\delta q = -0.461$ is transferred from D to A in the $S_0 \rightarrow S_1$ transition

	D ^a	C≡C	A ^b	C≡C	D
$q(S_0)$	0.154	-0.063	0.818	-0.063	0.154
$q(S_1)$	0.366	-0.044	0.357	-0.044	0.366
$\delta q = q(S_1) - q(S_0)$	0.212	0.019	-0.461	0.019	0.212

^a Electron donor (dimethylaminophenyl moiety). ^b Electron acceptor (azacyanine core).

observed solvent effects on the fluorescence spectra (blue shift with increasing polarity of the solvent). This effect is different from that typically observed for conventional ICT systems. In the light of the data given in Table 3, however it can be understood that the essence of these differences is associated with the multi-center character of the charge transfer in the V-shaped azacyanines in contrast to the two-center charge transfer between D and A in the case of typical ICT systems.

Finally, the data shown in Table S3† fit very well to the experimental results concerning the Stokes shifts, and even rate constants for radiative transition.

The rationale behind the surprisingly low fluorescence quantum yield for **4** can be found in the last column of Table S2.† The proximity of S₁ and T₂ states calculated for compound **4** establishes good conditions for a large intersystem crossing rate constant. At the same time, such conditions are not met for related bis(styryl)azacyanines²³ possessing large fluorescence quantum yields.

Two-photon absorption measurements

Two-photon absorption was measured for compounds **4** and **5** in DCM. It turned out that in contrast to what was observed previously for analogous dyes possessing a C–C double bond²³ as a linker, the two-photon absorption cross-section was significantly higher (at maxima) for dye **5** bearing the MeOC₆H₄ group ($\sigma_2 = 4200$ GM at 740 nm) while for dye **4** possessing a stronger electron-donating group it was only 47 GM at 740 nm. The effects associated with the internal charge transfer as well as in the geometry of linkers can be accounted for the difference in two photon absorption.

Conclusions

Cationic, conjugated chromophores, bearing a D– π –A⁺– π –D system, can be built in a straightforward manner from *N,N'*-methylene-2,2'-azapyridinocyanine as an electron-deficient core. The strongly polarized nature of these compounds is responsible for negative solvatochromism and for large differences in their linear optical properties. They have been designed in a way that the part of the molecule, which is responsible for high polarity, is also the integral part of the chromophore influencing optical properties. Most importantly, we have proved that the difference in the electron-donating ability between MeO and Me₂N groups has a significant influence on optical properties through determining intramolecular charge-transfer. The unusual hypsochromic shift of fluorescence with the increasing polarity of the solvent can be rationalized in terms of the multi-center character of the charge transfer in the V-shaped azacyanines (while in typical ICT systems it is two-center charge transfer between D and A). We also demonstrated that the two-photon absorption cross-section is higher for the dye possessing weaker electron-donating (*i.e.* methoxy) groups.

Experimental

Materials and methods

All commercially available compounds were used without additional purification, unless otherwise noted. Organic solvents were purified according to the generally accepted literature methods.³³ All the reported NMR spectra (¹H NMR and ¹³C NMR) were recorded on a Varian 500 spectrometer. High resolution mass spectra (HRMS) were obtained *via* electrospray (ESI). Chromatography was performed on silica gel 60 (230–400 mesh) and thin layer chromatography was performed on TLC plates (Merck, silica gel 60 F₂₅₄). Compound **1** was prepared according to a previously reported procedure.²⁶

Synthetic procedures

General method for the preparation of 3,9-bis(4-dimethylaminophenylethynyl)-6H-dipyrido[1,2-*a*:2',1'-*d'*][1,3,5]triazin-5-ium iodide (4**) and 3,9-bis(4-methoxyphenylethynyl)-6H-dipyrido[1,2-*a*:2',1'-*d'*][1,3,5]triazin-5-ium iodide (**5**).** A mixture of **1** (103 mg, 173 μ mol), copper(i) iodide (6.6 mg, 35 μ mol) and Pd(PPh₃)₂Cl₂ (13.8 mg, 17 μ mol) was dissolved in dry DMF (5 mL) in a Schlenk flask under an argon atmosphere. The phenylacetylene derivative (690 μ mol) was added, followed by dry Et₃N (135 μ L, 777 μ mol) and the resulting mixture was heated at 60 °C for 16 h. Then the solvent was removed and the dark residue was chromatographed (SiO₂, CH₂Cl₂/MeOH, 94 : 6). Fractions containing the desired product were evaporated and crystallized from *i*-PrOH, affording analytically pure samples.

4: dark violet crystals, 51 mg, 49%. ¹H NMR (DMSO, 500 MHz): δ 8.41 (d, *J* = 1.8 Hz, 2H), 8.05 (dd, *J* = 9.0, 1.8 Hz, 2H), 7.38, 6.74 (AA'BB', *J* = 8.9 Hz, 8H), 7.26 (d, *J* = 9 Hz, 2H), 6.40 (s, 2H), 2.97 (s, 12H). ¹³C NMR (DMSO, 125 MHz): δ 68.1, 84.8, 98.4, 110.1, 115.0, 115.7, 124.5, 135.7, 142.8, 147.6, 152.7, 153.7. HRMS (ESI): *m/z* calculated for C₃₁H₂₈IN₅ [M – I[−]] = 470.2345; found: 470.2356.

5: dark red crystals, 40 mg, 40%. ¹H NMR (DMSO, 500 MHz): δ 8.49 (d, *J* = 1.8 Hz, 2H), 8.10 (dd, *J* = 9.1, 1.8 Hz, 2H), 7.54, 7.04 (AA'BB', *J* = 8.5 Hz, 8H), 7.30 (d, *J* = 9.1 Hz, 2H), 6.42 (s, 2H), 3.82 (s, 6H). ¹³C NMR (DMSO, 125 MHz): δ 58.8, 69.2, 85.4, 96.7, 115.1, 116.2, 117.7, 124.6, 136.3, 143.5, 147.9, 153.1, 163.3. HRMS (ESI): *m/z* calculated for C₂₉H₂₂IN₃O₂ [M – I[−]] = 444.1712; found: 444.1714.

Linear optical measurements. Electronic absorption spectra were obtained on a UV-VIS absorption spectrometer Lambda 35 (Perkin Elmer, Rodgau, Germany). The spectra were corrected with solvent absorption spectra. Steady-state fluorescence emission spectra were obtained on an FLS920-stm spectrometer (Edinburgh Instruments, Livingston, United Kingdom). The spectra were corrected for the detector response. Fluorescence decays were also acquired on an FLS920-stm spectrometer using the Time Correlated Single Photon Counting (TCSPC) technique with a sub-nanosecond pulsed LED (EPLD 320) as an excitation source. Fluorescence decay times were determined from the decays using the least squares fitting method. The fitting was assumed to be correct when the goodness-of-fit value χ^2 was lower than 1.2. Fluor-

rescence quantum yields were measured on a C9920-02G absolute QY measurement system from Hamamatsu (Hamamatsu Photonics Deutschland GmbH, Herrsching am Ammersee, Germany). All measurements were executed using a 3 ml quartz cuvette (Hellma GmbH, Jena, Germany) with 1 cm light path. All measurements were executed for samples with an OD below 0.15.

Two-photon absorption measurements

The two-photon absorption (2PA) measurements were carried out using an FLS9020 fluorescence spectrometer (Edinburgh Instruments Ltd, Livingston, UK) equipped with an R928P photomultiplier (Hamamatsu, Japan) to detect the optical signal. Samples were measured in 1.0×1.0 cm quartz cuvettes in a 90° setup with direct excitation from a femtosecond (<100 fs) titan-sapphire-laser (Tsunami HP, Spectra Physics, Santa Clara, CA, USA) with 80 MHz repetition rate. The measurements were carried out in the wavelength range of 700 nm to 900 nm. The pulse spectrum (FWHM 10 nm) was monitored throughout the measurements by using a computer-controlled Avaspec-spectrometer (Avantes BV, Apeldoorn, NL). In order to focus the laser beam, an achromatic NIR-lens (Thorlabs GmbH, München, Germany) was integrated into the experimental setup along with a neutral density (ND) filter to adjust the average laser power (200 mW to 500 mW). The laser power was monitored by using an optical power meter right before starting any measurement. The spectral resolution was set to 1 nm, and differences in the signal intensity were compensated by adjusting the integration time (0.1 s to 2 s). The dye concentrations were varied between 9.0×10^{-7} M and 1.5×10^{-5} M, for optimal signal intensities, depending on the dye and solvent used.

Two-photon-excited fluorescence was used to determine the two-photon absorption cross-sections, σ_{2PA} (2PA-CS). Assuming that the fluorescence quantum yield under one- (Φ_1) and two-photon excitation (Φ_2) remains the same, two-photon excitation σ_{2PA} values were determined using the following equation⁴:

$$\sigma_{2PA}^P = \frac{c^S \cdot \Phi^S}{c^P \cdot \Phi^P} \cdot \frac{\int \lambda^P d\lambda}{\int \lambda^S d\lambda} \cdot \sigma_{2PA}^S$$

where σ_{2PA} is the two-photon absorption cross-section, c is the concentration, Φ is the quantum yield and $\int \lambda d\lambda$ corresponds to the field under a photoluminescence spectrum. The letters P and S denote the values determined for the probe and the standard (fluorescein), respectively. The σ_{2PA} values are given in Goeppert-Mayer (GM) units, where $1 \text{ GM} = 10^{-50} \text{ cm}^4 \text{ s per photon}$.

Theoretical calculations

All calculations were performed with the aid of the Gaussian 09 package.³⁴ Standard methods, DFT B3LYP/6-31G(d,p) and TDDFT B3LYP/6-31G(d,p) were used for the optimization of the molecular structures and calculations of the electronic transition energies. The effect of the solvent was included in

the polarizable-continuum model (PCM) with the use of the default options of this model implemented in the Gaussian.

Acknowledgements

The authors would like to kindly acknowledge financial support from the National Science Centre, Poland, grant MAESTRO-2012/06/A/ST5/00216 and the Foundation for Polish Science (TEAM-2009-4/3) and the Global Research Laboratory Program (2014K1A1A2064569) through the National Research Foundation (NRF) funded by Ministry of Science, ICT & Future Planning, Korea. Theoretical calculations were performed at the Interdisciplinary Center of Mathematical and Computer Modeling (ICM) of Warsaw University under the computational grant no. G-32-10.

Notes and references

- 1 M. Pawlicki, H. A. Collins, R. G. Denning and H. L. Anderson, *Angew. Chem.*, 2009, **121**, 3292–3316, (*Angew. Chem., Int. Ed.*, 2009, **48**, 3244–3266).
- 2 H. M. Kim and B. R. Cho, *Chem. Commun.*, 2009, 153–164.
- 3 G. S. He, L.-S. Tan, Q. Zheng and P. N. Prasad, *Chem. Rev.*, 2008, **108**, 1245–1330.
- 4 M. Rumi, S. Barlow, J. Wang, J. W. Perry and S. R. Marder, *Adv. Polym. Sci.*, 2008, **213**, 1–95.
- 5 (a) F. Terenziani, C. Katan, E. Badaeva, S. Tretiak and M. Blanchard-Desce, *Adv. Mater.*, 2008, **20**, 4641; (b) R. K. Tathavarty, M. Parent, M. H. V. Werts, S. Gmouh, A.-M. Caminade, L. Moreaux, S. Charpak, J.-P. Majoral and M. Blanchard-Desce, *Angew. Chem., Int. Ed.*, 2006, **45**, 4645; (c) M. H. V. Werts, N. Nerambourg, D. Pélégry, Y. Le Grand and M. Blanchard-Desce, *Photochem. Photobiol. Sci.*, 2005, **4**, 531; (d) C. Katan, S. Tretiak, M. H. V. Werts, A. J. Bain, R. J. Marsh, N. Leonczek, N. Nicolaou, E. Badaeva, O. Mongin and M. Blanchard-Desce, *J. Phys. Chem. B*, 2007, **111**, 9468.
- 6 C. Tang, Q. Zheng, H. Zhu, L. Wang, S.-C. Chen, E. Ma and X. Chen, *J. Mater. Chem. C*, 2013, **1**, 1771–1780.
- 7 F. Claeysens, E. A. Hasan, A. Gaidukeviciute, D. S. Achilleos, A. Ranella, C. Reinhardt, A. Ovsianikov, X. Shizhou, C. Fotakis, M. Vamvakaki, B. N. Chichkov and M. Farsari, *Langmuir*, 2009, **25**, 3219–3223.
- 8 D. A. Parthenopoulos and P. M. Renzepis, *Science*, 1989, **245**, 843–845.
- 9 C. C. Corredor, Z.-L. Huang, K. D. Belfield, A. R. Morales and M. V. Bondar, *Chem. Mater.*, 2007, **19**, 5165–5173.
- 10 E. J. C. Diaz, S. Picard, V. Chevasson, J. Daniel, V. Hugues, O. Mongin, E. Genin and M. Blanchard-Desce, *Org. Lett.*, 2015, **17**, 102–105.
- 11 (a) K. D. Belfield, M. V. Bondar, S. Yao, I. A. Mikhailov, V. S. Polikanov and O. V. Przhonska, *J. Phys. Chem. C*, 2014, **118**, 13790–13800; (b) K. D. Belfield, C. D. Andrade, C. O. Yanez, M. V. Bondar, F. E. Hernandez and

- O. V. Przhonska, *J. Phys. Chem. B*, 2010, **114**, 14087–14095; (c) H. M. Kim and B. R. Cho, *Acc. Chem. Res.*, 2009, **42**, 863–872; (d) A. S. Rao, D. Kim, H. Nam, H. Jo, K. H. Kim, C. Ban and K. H. Ahn, *Chem. Commun.*, 2012, **48**, 3206–3208; (e) H.-Y. Ahn, K. E. Fairfull-Smith, B. J. Morrow, V. Lussini, B. Kim, M. V. Bondar, S. E. Bottle and K. D. Belfield, *J. Am. Chem. Soc.*, 2012, **134**, 4721–4730; (f) S. K. Lee, W. J. Yang, J. J. Choi, C. H. Kim, S.-J. Jeon and B. R. Cho, *Org. Lett.*, 2005, **7**, 323–326; (g) X. Wang, D. M. Nguyen, C. O. Yanez, L. Rodriguez, H.-Y. Ahn, M. V. Bondar and K. D. Belfield, *J. Am. Chem. Soc.*, 2010, **132**, 12237–12239; (h) A. R. Morales, K. J. Schafer-Hales, A. I. Marcus and K. D. Belfield, *Bioconjugate Chem.*, 2008, **19**, 2559–2567; (i) H. Yao, H.-Y. Ahn, X. Wang, J. Fu, E. W. Van Stryland, D. J. Hagan and K. D. Belfield, *J. Org. Chem.*, 2010, **75**, 3965–3974; (j) B. R. Cho, M. J. Piao, K. H. Son, H. L. Sang, J. Y. Soo, S.-J. Jeon and M. Cho, *Chem. – Eur. J.*, 2002, **8**, 3907–3916.
- 12 A. Ustione and D. W. Piston, *J. Microsc.*, 2011, **243**, 221–226.
- 13 T. K. Ahn, K. S. Kim, D. Y. Kim, S. B. Noh, N. Aratani, C. Ikeda, A. Osuka and D. Kim, *J. Am. Chem. Soc.*, 2006, **128**, 1700–1704.
- 14 H. A. Collins, M. Khurana, E. H. Moriyama, A. Mariampillai, E. Dahlstedt, M. Balaz, M. K. Kuimova, M. Drobizhev, V. X. D. Yang, D. Phillips, A. Rebane, B. C. Wilson and H. L. Anderson, *Nat. Photonics*, 2008, **2**, 420–424.
- 15 M. Williams-Harry, A. Bhaskar, G. Ramakrishna, T. Goodson, III, M. Imamura, A. Mawatari, K. Nakao, H. Enozawa, T. Nishinaga and M. Iyoda, *J. Am. Chem. Soc.*, 2008, **130**, 3252–3253.
- 16 S. Kim, Q. Zheng, G. S. He, D. J. Bharali, H. E. Pudavar, A. Baev and P. N. Prasad, *Adv. Funct. Mater.*, 2006, **16**, 2317–2323.
- 17 S.-J. Chung, S. Zheng, T. Odani, L. Beverina, J. Fu, L. A. Padilha, A. Biesso, J. M. Hales, X. Zhan, K. Schmidt, A. Ye, E. Zojer, S. Barlow, D. J. Hagan, E. W. Van Stryland, Y. Yi, Z. Shuai, G. A. Pagani, J.-L. Brédas, J. W. Perry and S. R. Marder, *J. Am. Chem. Soc.*, 2006, **128**, 14444–14445.
- 18 H. M. Kim, P. R. Yang, M. S. Seo, J. S. Yi, J. H. Hong, S. J. Jeon, Y. G. Ko, K. J. Lee and B. R. Cho, *J. Org. Chem.*, 2007, **72**, 2088–2096.
- 19 A. Nowak-Król, M. Grzybowski, J. Romiszewski, M. Drobizhev, G. Wicks, M. Chotkowski, A. Rebane, E. Górecka and D. T. Gryko, *Chem. Commun.*, 2013, **49**, 8368–8370.
- 20 M. Grzybowski, V. Hugues, M. Blanchard-Desce and D. T. Gryko, *Chem. – Eur. J.*, 2014, **20**, 12493–12501.
- 21 Y. M. Poronik, V. Hugues, M. Blanchard-Desce and D. T. Gryko, *Chem. – Eur. J.*, 2012, **18**, 9258–9266.
- 22 (a) M. A. Ramírez, A. M. Cuadro, J. Alvarez-Builla, O. Castaño, J. L. Andrés, F. Mendicuti, K. Clays, I. Asselberghs and J. J. Vaquero, *Org. Biomol. Chem.*, 2012, **10**, 1659–1669; (b) E. Maçôas, G. Marcelo, S. Pinto, T. Cañeque, A. M. Cuadro, J.-J. Vaquero and J. M. G. Martinho, *Chem. Commun.*, 2011, **47**, 7374–7376; (c) M. A. Ramirez, T. Cañeque, A. M. Cuadro, F. Mendicuti, K. Clays, I. Asselbergh and J. J. Vaquero, *ARKIVOC*, 2011, **iii**, 140–155; (d) T. Cañeque, A. M. Cuadro, J. Alvarez-Builla, J. Pérez-Moreno, K. Clays, G. Marcelo, F. Mendicuti, O. Castaño, J. L. Andrés and J. J. Vaquero, *Eur. J. Org. Chem.*, 2010, 6323–6330; (e) A. Nuñez, B. Abarca, A. M. Cuadro, J. Alvarez-Builla and J. J. Vaquero, *J. Org. Chem.*, 2009, **74**, 4166–4176; (f) A. Nuñez, A. M. Cuadro, J. Alvarez-Builla and J. J. Vaquero, *Org. Lett.*, 2007, **9**, 2977–2980; (g) D. García-Cuadrado, A. M. Cuadro, B. M. Barchín, A. Nuñez, T. Cañeque, J. Alvarez-Builla and J. J. Vaquero, *J. Org. Chem.*, 2006, **71**, 7989–7995; (h) D. García-Cuadrado, A. M. Cuadro, J. Alvarez-Builla, U. Sancho, O. Castaño and J. J. Vaquero, *Org. Lett.*, 2006, **8**, 5955–5958; (i) D. Garcia-Cuadrado, A. M. Cuadro, J. Alvarez-Builla and J. J. Vaquero, *Org. Lett.*, 2004, **6**, 4175–4178.
- 23 M. Tasiar, V. Hugues, M. Blanchard-Desce and D. T. Gryko, *Asian J. Org. Chem.*, 2013, **2**, 669–673.
- 24 S. Munavalli, F.-L. Hsu and E. Poziomek, *Heterocycles*, 1986, **24**, 1893.
- 25 J. M. Haddadin, M. J. Kurth and M. M. Olmstead, *Tetrahedron Lett.*, 2000, **41**, 5613–5616.
- 26 K. S. Huang, M. J. Haddadin, M. M. Olmstead and M. J. Kurth, *J. Org. Chem.*, 2001, **66**, 1310–1315.
- 27 D. Patra, N. N. Malaeb, M. J. Haddadin and M. J. Kurth, *J. Fluoresc.*, 2012, **22**, 707–717.
- 28 H. Meier, *Angew. Chem., Int. Ed.*, 2005, **44**, 2482–2506.
- 29 O. Mongin, L. Porrès, M. Charlot, C. Katan and M. Blanchard-Desce, *Chem. – Eur. J.*, 2007, **13**, 1481–1498.
- 30 J. O. Morley, R. M. Morley, R. Docherty and M. H. Charlton, *J. Am. Chem. Soc.*, 1997, **119**, 10192–10202.
- 31 A. Mielniczak, B. Wandelt and S. Wysocki, *Mater. Sci.*, 2002, **20**, 59–68.
- 32 C. Jamorski-Jödicke and H.-P. Lüthi, *J. Chem. Phys.*, 2002, **117**, 4146.
- 33 W. L. F. Armarego and C. L. L. Chai, *Purification of Laboratory Chemicals*, Elsevier Science, 4th edn, 2003.
- 34 See the ESI† for more details.